

GEOMETRICALLY NONLINEAR ANALYSIS OF IMPERFECT LAMINATED COMPOSITE PLATES WITH A VARIABLE FIBER SPACING

Ali I. Al-Mosawi
 Technical Institute-Babylon
 Lecturer

ABSTRACT

The primary objective of research is to determine the improved structural efficiency of plates can be with variable fiber spacing. The Post-buckling of laminated composite plate with variable fiber spacing is obtained numerically, using eight node isoparametric quadrilateral elements (serendipity element) with five degree of freedom per node. The mathematical formulation is based on first-order shear deformation theory and von-Karman non-linearity. The effect of the initial geometric imperfection, fiber spacing, orientation fiber, and direction of in-plane loading were considered. Numerical results for boron/Epoxy fiber reinforced laminates are presented for the different effects of the composite plate under in-plane loading. This study showed that the post buckling behavior of composite plate very sensitive for type of distribution fiber and the seventh distribution equation gives maximum buckling load and smallest deformation.

KEYWORDS: Post-Buckling Behavior, Composite Laminated, Fiber Spacing

- /

.(von-Karman)

(/)

INTRODUCTION

Composite laminates have been developed and utilized because of its outstanding bending rigidity, low specific weight, superior isolating qualities, excellent vibration characteristics and good fatigue properties. The first two characteristics are the major reasons to make it use more often in aerospace vehicles that need high strength-to-weight ratio. Thin-walled structures are often designed to carry compressive loads not only until an initial buckling load but also far beyond it: in a post buckling regime. In these problems, the initial buckling load of the plate elements, as well as the stiffness and strength of the structures in the post buckling phase are critical considerations in the design process. Buckling and post buckling resistance can be increased by various optimization methods. Optimization is a common approach in designing structures made of composites, since these materials can be easily adapted to a given situation. The most common optimization techniques include a variation of fiber directions, ply thickness and stacking sequences. However, it is possible that significant increases in structural efficiency may be obtained by varying the fiber spacing--packing them closely together in regions where great stiffness is needed, but less densely in other regions [Sheh and Le, 2009].

Martin and Leissa investigated the plane stress problem of a rectangular of composite sheet with variable fiber content [Martin and Leissa, 1989]. The single layer composite having fibers parallel to the edges are macroscopically orthotropic, but non homogeneous. The stresses obtained from this analysis were treated as input to the first vibration and buckling study of composites with variable fiber spacing [Leissa and Martin, 1990]. Numerical results are obtained for six nonuniform distributions of glass, graphite and boron fibers. The redistribution may increase the buckling load by as much as 38%. Leissa and Martin [Leissa and Martin, 1990] also presented exact solutions for the stress, strain and displacement fields for four types of problems with arbitrary fiber spacing. Shiau and Chue [Shiau and Chue, 1991] also used a similar concept to reduce the free edge interlaminar stresses.

By varying the fiber volume fraction near the free edge, the interlaminar normal and shear stresses near the free edges can be significantly reduced. Shiau and Lee [Shiau and Chue, 1993] studied stress concentration around holes in composite laminates with variable fiber spacing. An 18 degree of freedom higher-order triangular plane stress element was developed to investigate the effect of variable fiber spacing on the stress concentration around a hole in a composite laminated plate subjected to in-plane boundary loadings. It proves that reducing the fiber volume ratio near the edges of hole can significantly reduce the stress concentration in that region. It is interesting to note that the higher fiber volume fraction may increase the buckling load of the plate. The stress concentration is also more obvious in the region with higher fiber volume fraction. Recently, Sheh-Yao and Le-Shiau [Sheh and Le, 2009] studied Buckling and vibration of composite laminated plates with variable fiber spacing by use finite element method. The formulation of the location-dependent stiffness matrix due to non homogeneous material properties was derived. They concluded that the more fibers distributed in the central portion of the plate may efficiently increase the buckling load and natural frequencies. The fibers distributed in the outer portion of the plate may increase the critical buckling load. So, they concluded that the natural frequencies decreased due to increasing more mass than stiffness where the fiber distribution may change the stiffness and mass of the plate.

So, the present study is the first to treat the post buckling problems for composite plates having variable fiber spacing. The primary objective is to determine whether the structural efficiency of plates can be improved with variable fiber spacing. Initial imperfection, fiber angle, and direction of load, were considered in the present study.

FORMULATION OF COMPOSITE LAMINATED PLATES

Consider a composite laminated plate with length a , width b and thickness h , using Mindlin formulation, the gross displacements $\mathbf{u} = [\mathbf{u} \quad \mathbf{v} \quad \mathbf{w}]^T$ at (x,y,z) are expressed as functions of the mid plane translations $\hat{u}, \hat{v}, \hat{w}$ and independent normal rotations θ_x and θ_y [Pica, Wood and Hinton, 1979].

$$\begin{aligned} u &= \hat{u}(x, y) - z\theta_x(x, y) \\ v &= \hat{v}(x, y) - z\theta_y(x, y) \\ w &= \hat{w}_o(x, y) + w_1(x, y) \end{aligned} \tag{1}$$

θ_x and θ_y , are the rotations of the normals, to the undeformed midplane, in the xz and yz planes respectively. These normals are not necessarily normal to the mid plane after deformation and consequently shear deformation is permitted, w and w_1 equal the mid plane initial and net deformations in the z -direction, respectively $\bar{w}_o(x, y)$, $w_1(x, y)$, see **Figure 1**.

For a Mindlin plate theory, the relevant midplane Green's strain vector is revised to give [**Pica, Wood and Hinton, 1979**]:

$$\boldsymbol{\varepsilon} = \begin{Bmatrix} \varepsilon_x \\ \varepsilon_y \\ \gamma_{xy} \\ \gamma_{xz} \\ \gamma_{yz} \end{Bmatrix} = \begin{Bmatrix} \frac{\partial u}{\partial x} + \frac{1}{2} \left(\frac{\partial u}{\partial x} \right)^2 + \frac{1}{2} \left(\frac{\partial v}{\partial x} \right)^2 + \frac{1}{2} \left(\frac{\partial w}{\partial x} \right)^2 \\ \frac{\partial v}{\partial y} + \frac{1}{2} \left(\frac{\partial u}{\partial y} \right)^2 + \frac{1}{2} \left(\frac{\partial v}{\partial y} \right)^2 + \frac{1}{2} \left(\frac{\partial w}{\partial y} \right)^2 \\ \frac{\partial u}{\partial y} + \frac{\partial v}{\partial x} + \frac{\partial u}{\partial x} \cdot \frac{\partial u}{\partial y} + \frac{\partial v}{\partial x} \cdot \frac{\partial v}{\partial y} + \frac{\partial w}{\partial x} \cdot \frac{\partial w}{\partial y} \\ \frac{\partial u}{\partial z} + \frac{\partial w}{\partial x} + \frac{\partial u}{\partial x} \cdot \frac{\partial u}{\partial z} + \frac{\partial v}{\partial x} \cdot \frac{\partial v}{\partial z} + \frac{\partial w}{\partial x} \cdot \frac{\partial w}{\partial z} \\ \frac{\partial v}{\partial z} + \frac{\partial w}{\partial y} + \frac{\partial u}{\partial y} \cdot \frac{\partial u}{\partial z} + \frac{\partial v}{\partial y} \cdot \frac{\partial v}{\partial z} + \frac{\partial w}{\partial y} \cdot \frac{\partial w}{\partial z} \end{Bmatrix} - \begin{Bmatrix} \frac{1}{2} \left(\frac{\partial w_o}{\partial x} \right)^2 \\ \frac{1}{2} \left(\frac{\partial w_o}{\partial y} \right)^2 \\ \frac{\partial w_o}{\partial x} \cdot \frac{\partial w_o}{\partial y} \\ \frac{\partial w_o}{\partial x} + \frac{\partial w_o}{\partial x} \cdot \frac{\partial w_o}{\partial z} \\ \frac{\partial w_o}{\partial y} + \frac{\partial w_o}{\partial y} \cdot \frac{\partial w_o}{\partial z} \end{Bmatrix} \quad (2)$$

Introducing the von-Karman assumptions which imply that derivatives of u and v with respect to x, y and z are small and noting that w is independent of z allows Green's strain to be rewritten in terms of the mid plane deformations of Equation(1), as [**Pica, Wood and Hinton, 1979**]:

$$\boldsymbol{\varepsilon} = \begin{Bmatrix} \varepsilon_x \\ \varepsilon_y \\ \gamma_{xy} \\ \gamma_{xz} \\ \gamma_{yz} \end{Bmatrix} = \begin{Bmatrix} \boldsymbol{\varepsilon}_p^o \\ \mathbf{0} \end{Bmatrix} + \begin{Bmatrix} z \boldsymbol{\varepsilon}_b^o \\ \boldsymbol{\varepsilon}_s^o \end{Bmatrix} + \begin{Bmatrix} \boldsymbol{\varepsilon}_p^I \\ \mathbf{0} \end{Bmatrix} + \begin{Bmatrix} \boldsymbol{\varepsilon}_p^L \\ \mathbf{0} \end{Bmatrix} \quad (3)$$

where the linear midplane strains are:

The in-plane strain

$$\boldsymbol{\varepsilon}_p^o = \begin{Bmatrix} \frac{\partial \bar{u}}{\partial x} \\ \frac{\partial \bar{v}}{\partial y} \\ \frac{\partial \bar{u}}{\partial y} + \frac{\partial \bar{v}}{\partial x} \end{Bmatrix} \quad (4a)$$

The bending strain:

$$\boldsymbol{\varepsilon}_b^o = \begin{Bmatrix} \frac{\partial \theta_x}{\partial x} \\ \frac{\partial \theta_y}{\partial y} \\ \frac{\partial \theta_x}{\partial y} + \frac{\partial \theta_y}{\partial x} \end{Bmatrix} \quad (4b)$$

And the shear strain

$$\boldsymbol{\varepsilon}_s^o = - \left\{ \begin{array}{l} \frac{\partial \widehat{w}_x}{\partial x} - \theta_x \\ \frac{\partial \widehat{w}_x}{\partial y} - \theta_y \end{array} \right\} \quad (4c)$$

The linear contribution of the initial deformation to the in plane strain:

$$\boldsymbol{\varepsilon}_p^I = \left\{ \begin{array}{l} \frac{\partial \widehat{w}_o}{\partial x} \cdot \frac{\partial \widehat{w}_1}{\partial x} \\ \frac{\partial \widehat{w}_o}{\partial y} \cdot \frac{\partial \widehat{w}_1}{\partial y} \\ \frac{\partial \widehat{w}_o}{\partial x} \cdot \frac{\partial \widehat{w}_1}{\partial y} + \frac{\partial \widehat{w}_o}{\partial y} \cdot \frac{\partial \widehat{w}_1}{\partial x} \end{array} \right\} \quad (4d)$$

And finally the nonlinear component of in plane strain;

$$\boldsymbol{\varepsilon}_p^L = - \left\{ \begin{array}{l} \frac{1}{2} \left(\frac{\partial \widehat{w}}{\partial x} \right)^2 \\ \frac{1}{2} \left(\frac{\partial \widehat{w}}{\partial y} \right)^2 \\ \frac{\partial \widehat{w}}{\partial x} \cdot \frac{\partial \widehat{w}}{\partial y} \end{array} \right\} \quad (4e)$$

The vector components of Equation (4), represent the generalized strains. It can be noticed that the vector $\boldsymbol{\varepsilon}_p^o + \boldsymbol{\varepsilon}_p^I + \boldsymbol{\varepsilon}_p^L$ reproduces the Marguerre strain expression for moderately thick plate.

The basis of the formulation is the virtual work equation for a continuum written in a total Lagrangian coordinate system under the assumption of small strains and conservative loading as [Pica and Wood, 1980]:

$$\int_V d\boldsymbol{\varepsilon}^T \boldsymbol{\sigma} dv = \int_V \rho d\mathbf{u}^T \mathbf{q} dv + \int_A d\mathbf{u}^T \mathbf{p} dA \quad (5)$$

where V is the undeformed volume, \mathbf{u} the Piola-Kirchhoff stress vector, $d\boldsymbol{\varepsilon}$ the virtual Green's strain vector due to the virtual displacements $d\mathbf{u}$, ρ the mass density, \mathbf{q} the body forces per unit mass and \mathbf{p} surface tractions acting over an undeformed area A .

For the plate formulation this virtual work equation is to be rewritten in terms of area integrals over the midsurface. The internal virtual work dW_i can be written as an integral over the plate area A and thickness t as,

$$dW_i = \int_V d\boldsymbol{\varepsilon}^T \boldsymbol{\sigma} dv = \int_A \int_{-h/2}^{h/2} (d\boldsymbol{\varepsilon}_x \boldsymbol{\sigma}_x + d\boldsymbol{\varepsilon}_y \boldsymbol{\sigma}_y + d\boldsymbol{\gamma}_{xy} \boldsymbol{\tau}_{xy} + d\boldsymbol{\gamma}_{xz} \boldsymbol{\tau}_{xz} + d\boldsymbol{\gamma}_{yz} \boldsymbol{\tau}_{yz}) dz \cdot dA \quad (6)$$

Substituting the strain expression from Equation (3) into equation (6) and integrating over the thickness allows dW_i to be rewritten only as an area integral giving,

$$dW_i = \int_A d\hat{\varepsilon}^T \hat{\sigma} dA \quad (7)$$

In which the resultant vector $\hat{\sigma}$ is,

$$\hat{\sigma} = \begin{Bmatrix} \sigma_p \\ \sigma_b \\ \sigma_o \end{Bmatrix} \quad (8)$$

which contains the following components, in-plane

$$\hat{\sigma}_p = [N_x \quad N_y \quad N_{xy}]^T = \int_{-h/2}^{h/2} [\sigma_x \quad \sigma_y \quad \tau_{xy}] dz \quad (9)$$

$$\hat{\sigma}_b = [M_x \quad M_y \quad M_{xy}]^T = \int_{-h/2}^{h/2} [\sigma_x \quad \sigma_y \quad \tau_{xy}] z dz \quad (10)$$

Shear,

$$\hat{\sigma}_s = [Q_x \quad Q_y]^T = \int_{-h/2}^{h/2} [\tau_{xz} \quad \tau_{yz}] dz \quad (11)$$

The second integral in Equation (6) which represents the external virtual work due to body forces may be rewritten as [Pica and Wood,1980],

$$dW_{ex}^b = \int_A \int_{-h/2}^{h/2} \rho (duq_x + dvq_y + dwq_z) dz.dA \quad (12)$$

Substituting for u , v and w from Equation (1) and integrating explicitly through the thickness allows equation (12) to be expressed as an area integral giving,

$$dW_{ex}^b = \int_A d\hat{u}^T \hat{q} dA \quad (13)$$

Where the midplane displacement vector \hat{u} is,

$$\hat{u} = [\hat{u} \quad \hat{v} \quad \hat{w} \quad \theta_x \quad \theta_y]^T \quad (14)$$

And the generalized body force vector \hat{q} is,

$$\hat{q} = [\hat{q}_x \quad \hat{q}_y \quad \hat{q}_z \quad \hat{M}_x \quad \hat{M}_y]^T = \int_{-h/2}^{h/2} \rho (q_x \quad q_y \quad q_z \quad -q_x z \quad -q_y z) dz \quad (15)$$

If the body force vector ρq is constant over thickness, \hat{q} becomes simply;

$$\hat{q} = [\rho q_x t \quad \rho q_y t \quad \rho q_z t \quad 0 \quad 0]^T \quad (16)$$

where typically ρq_x is the force per unit area in the x direction. Finally the third integral of equation (5) which represents the external virtual work due to tractions may be split into two terms relating to the plate surfaces ($A_s, z = \pm t/2$, and the plate edges (a_e), see **Figure 2**, as,

$$dW_{ex}^t = \int_{A_s} du^t P dA + \int_{A_e} du^t P_e dA \quad (17)$$

where the tractions on the surfaces $z = \pm t/2$ are,

$$P = \{P_x \quad P_y \quad P_z\}^T \quad (18)$$

and the global edge tractions P_e are given in terms of the local edge tractions P_x, P_y and P_z as,

$$P_e = \begin{Bmatrix} P_x^e \\ P_y^e \\ P_z^e \end{Bmatrix} = \begin{bmatrix} c & s & 0 \\ s & c & 0 \\ 0 & 0 & 1 \end{bmatrix} \begin{Bmatrix} P_n \\ P_t \\ P_z \end{Bmatrix} \quad (19)$$

where $c = \cos\theta$ and $s = \sin\theta$, see **Figure 2**.

Substituting for u, v and w from equation (1) into equation (17) and integrating the edge area integral explicitly through the thickness gives the work term dW_{ex}^t , as the sum of an area integral over (a) and a line integral over an edge length s .

$$dW_{ex}^t = \int_{A_s} d\hat{u}^T \hat{P} dA + \int_s d\hat{u}^T \hat{P}_e ds \quad (20)$$

where

$$\hat{P} = \{P_x \quad P_y \quad P_z \quad M_x \quad M_y\}^T \quad (21)$$

The generalized edge forces are:

$$\hat{P}_e = \{\hat{P}_x^e \quad \hat{P}_y^e \quad \hat{P}_z^e \quad \hat{M}_x^e \quad \hat{M}_y^e\}^T = \begin{bmatrix} \int_{-t/2}^{t/2} P_x^e & P_y^e & P_z^e & -P_x^e z & -P_y^e z \end{bmatrix}^T \quad (22)$$

The virtual work equation (17) may now be written entirely in terms of ‘‘mid plane’’ quantities as,

$$\int_A d\hat{\varepsilon}^T \hat{\sigma} dA = \int_A \rho d\hat{u}^T \hat{q} dv + \int_{a_s} d\hat{u}^T \hat{p} dA + \int_s d\hat{u}^T \hat{p}_e ds \quad (23)$$

The plate is assumed to consist of N layers of orthotropic sheets bonded together. Each layer has arbitrary fiber orientation. The fibers in each layer are aligned parallel to the longitudinal direction but distributed unevenly in the transverse direction. Hence, the fiber volume fraction, V_f , is a function of nondimensional coordinate x having its origin at the plate edge of plate as shown in **Figure 3**. Suppose, for example, the fibers are aligned parallel to the x direction and the fiber volume fraction varies parabolically

as $V_f(x) = \left(\frac{4}{L} x - \frac{4}{L^2} x^2 \right)$. The material is all fiber at the plate center ($x = a/2$), whereas at the edges ($x = 0, a$), it is all matrix. With this variable fiber spacing, the elastic modulus $E_1, E_2, \nu_{12}, G_{12}$ for the composite material are also the functions of x . In this study, the formulas used for the calculation of these effective engineering constants are based on the rule of mixture [Sheh and Le, 2009].

$$\begin{aligned}
 E_1(x) &= E_f V_f(x) + E_m (1 - V_f(x)) \\
 E_2(x) &= \frac{E_f E_m}{E_f (1 - V_f(x)) + E_m V_f(x)} \\
 \nu_{12}(x) &= \nu_f V_f(x) + \nu_m (1 - V_f(x)) \\
 G_{12}(x) &= \frac{G_f G_m}{G_f (1 - V_f(x)) + G_m V_f(x)}
 \end{aligned}
 \tag{24}$$

The stress–strain relation for the orthotropic sheet with variable fiber spacing can be expressed as:

$$\begin{bmatrix} \sigma_1 \\ \sigma_2 \\ \tau_{12} \end{bmatrix}^L = \begin{bmatrix} Q_{11}(x) & Q_{12}(x) & 0 \\ Q_{12}(x) & Q_{22}(x) & 0 \\ 0 & 0 & Q_{66}(x) \end{bmatrix} \begin{Bmatrix} \varepsilon_1 \\ \varepsilon_2 \\ \gamma_{12} \end{Bmatrix}
 \tag{25}$$

Where :

$$\begin{aligned}
 Q_{11}(x) &= \frac{E_1(x)}{(1 - \nu_{12}(x)\nu_{21}(x))} \\
 Q_{12}(x) &= \frac{\nu_{12}(x)E_1(x)}{(1 - \nu_{12}(x)\nu_{21}(x))} \\
 Q_{22}(x) &= \frac{E_2(x)}{(1 - \nu_{12}(x)\nu_{21}(x))} \\
 Q_{66}(x) &= G_{12}(x)
 \end{aligned}
 \tag{26}$$

For a composite laminated plate with N layers, the stress–strain relation of k th layer of the plate can be expressed as:

$$\{\sigma\}_k = [Q]_k \{\varepsilon\}
 \tag{27}$$

where Q_{ij} are the transformed reduced stiffness. Now the stress–strain relation becomes location dependent. The force and moment resultants of the composite laminated plate are defined as [Phan, and Reddy, 1985]:

$$[N] = \begin{bmatrix} N_x & N_y & N_{xy} \end{bmatrix}^L = \int_{-h/2}^{h/2} \begin{bmatrix} \sigma_x & \sigma_y & \tau_{xy} \end{bmatrix} dz
 \tag{28}$$

$$[M] = \begin{bmatrix} M_x & M_y & M_{xy} \end{bmatrix}^L = \int_{-h/2}^{h/2} \begin{bmatrix} \sigma_x & \sigma_y & \tau_{xy} \end{bmatrix} z dz
 \tag{29}$$

which leads to,

$$\begin{aligned}
 \{N\} &= [A] \{\varepsilon_o\} \\
 \{M\} &= [D] \{\kappa\}
 \end{aligned}
 \tag{30}$$

where the extensional rigidity [A] and bending rigidity [D] of the panel are defined as:

$$A_{ij} = \sum_{k=1}^N Q_{ij} (h_k - h_{k-1}) \quad i, j = 1, 2, 6
 \tag{31}$$

$$D_{ij} = \frac{1}{3} \sum_{k=1}^N Q_{ij} (h_k^3 - h_{k-1}^3) \quad i, j = 1, 2, 6
 \tag{32}$$

Before proceeding with the discretisation of the virtual work equation (23), it is necessary to consider further the variation of strain du due to the virtual displacements $d\hat{\epsilon}$. Generally $d\hat{\epsilon}$ is given as the sum of the variation of the linear and nonlinear generalized strains as [Sheh and Le, 2009]:

$$d\hat{\epsilon} = d\hat{\epsilon}^o + d\hat{\epsilon}^L \tag{33}$$

$$d\hat{\epsilon}^o = \begin{bmatrix} \frac{\partial}{\partial x} & 0 & 0 & 0 & 0 \\ 0 & \frac{\partial}{\partial y} & 0 & 0 & 0 \\ \frac{\partial}{\partial y} & \frac{\partial}{\partial x} & 0 & 0 & 0 \\ 0 & 0 & 0 & -\frac{\partial}{\partial x} & 0 \\ 0 & 0 & 0 & 0 & -\frac{\partial}{\partial y} \\ 0 & 0 & 0 & -\frac{\partial}{\partial y} & -\frac{\partial}{\partial x} \\ 0 & 0 & \frac{\partial}{\partial x} & -1 & 0 \\ 0 & 0 & \frac{\partial}{\partial y} & 0 & -1 \end{bmatrix} d \begin{Bmatrix} \hat{u} \\ \hat{v} \\ \hat{w} \\ \theta_x \\ \theta_y \end{Bmatrix} \tag{34}$$

If the displacement gradients with respect to the lateral displacements \hat{w} are,

$$\theta = \begin{bmatrix} \frac{\partial \hat{w}}{\partial x} & \frac{\partial \hat{w}}{\partial y} \end{bmatrix}^T \tag{35}$$

$$\hat{w} = w + w_o$$

Where :

w_o =initial deflection .

Then the variation of the nonlinear component of the inplane strain is obtained from equation (4e) in terms of the virtual gradients $d\theta$ as,

$$d\hat{\epsilon}_p^L = A_\theta d\theta \tag{36}$$

where

$$A_\theta = \begin{bmatrix} \frac{\partial \hat{w}}{\partial x} & 0 \\ 0 & \frac{\partial \hat{w}}{\partial y} \\ \frac{\partial \hat{w}}{\partial y} & \frac{\partial \hat{w}}{\partial x} \end{bmatrix} \tag{37}$$

And,

$$d\theta = d \begin{bmatrix} \frac{\partial \hat{w}}{\partial x} & \frac{\partial \hat{w}}{\partial y} \end{bmatrix}^T \tag{38}$$

May now be written in terms of the nodal displacements (u) and Cartesian derivatives of the shape functions as:

$$d\theta = [G] du \tag{39}$$

where

$$[G] = [G_1 \quad G_2 \quad G_3 \quad G_n] \quad (40)$$

and,

$$G_i = \begin{bmatrix} 0 & 0 & \frac{\partial N_i}{\partial x} & 0 & 0 \\ 0 & 0 & \frac{\partial N_i}{\partial y} & 0 & 0 \end{bmatrix} \quad (41)$$

The above equation represents the gradient for five degrees of freedom per node. The generalized Green's strain vector of equation (33) is given in terms of nodal displacements u , displacement gradients A_0 and Cartesian derivatives of N as [Pica and Wood, 1980],

$$\hat{\varepsilon} = \left[B_o + \frac{1}{2} B_L(u) \right] u \quad (42)$$

where B_o is the strain matrix giving the linear strains ε_p^o , ε_b^o and ε_s^o and B_L , which is linearly dependent upon u , gives the nonlinear strains ε_p^L . Consequently the nonlinear strains are quadratically dependent upon the nodal displacements u .

The constant matrix B_o is written in terms of nodal sub matrices as,

$$B_o = [B_{o1}, B_{o2}, \dots, B_{on}] \quad (43)$$

Where

$$B_o = \begin{bmatrix} B_{oi}^p & \mathbf{0} \\ \mathbf{0} & B_{oi}^b \\ \mathbf{0} & B_{oi}^s \end{bmatrix} \quad (44)$$

In which component matrices are in-plane matrix

$$B_{oi}^p = \begin{bmatrix} \frac{\partial N_i}{\partial x} & \mathbf{0} \\ \mathbf{0} & \frac{\partial N_i}{\partial y} \\ \frac{\partial N_i}{\partial y} & \frac{\partial N_i}{\partial x} \end{bmatrix} \quad (45)$$

Bending matrix

$$B_{oi}^b = \begin{bmatrix} \mathbf{0} & -\frac{\partial N_i}{\partial x} & \mathbf{0} \\ \mathbf{0} & \mathbf{0} & -\frac{\partial N_i}{\partial y} \\ \mathbf{0} & -\frac{\partial N_i}{\partial y} & -\frac{\partial N_i}{\partial x} \end{bmatrix} \quad (46)$$

And then shear matrix

$$B_{oi}^s = \begin{bmatrix} \frac{\partial N_i}{\partial x} & -N_i & 0 \\ \frac{\partial N_i}{\partial y} & 0 & N_i \end{bmatrix} \quad (47)$$

The strain matrix B_L consists of the nodal sub matrices

$$B_L = [B_{L1} \quad B_{L2} \quad \dots \quad B_{Ln}] \quad (48)$$

Where

$$B_{Li} = \begin{bmatrix} A_\theta \\ 0 \\ 0 \end{bmatrix} G_i \quad (49)$$

The strain variation in terms of the virtual nodal displacements du as,

$$d\hat{\epsilon} = Bdu \quad (50)$$

In which

$$B = B_o + B_L \quad (51)$$

The virtual work equation (23) is discretised, for an element, by substituting becomes as [Pica and Wood, 1980],

$$\left[\int_A B^T \hat{\sigma} dA - R \right] du = 0 \quad (52)$$

where the equivalent nodal load vector R due to body forces and tractions is,

$$R = \int_A N^T \hat{q} dA + \int_{As} N^T \hat{P} dA + \int_s N^T \hat{P}_e ds \quad (53)$$

Since the nodal virtual displacements du is arbitrary the element nonlinear equilibrium equations become,

$$\psi(u) = \int_A B^T \hat{\sigma} dA - R = 0 \quad (54)$$

The load vector R may also contain nodal point loads. Equation (54) can have the dual role of representing either the element, or in an assembled form the total equilibrium equation. It is a nonlinear equation in u since B and $\hat{\sigma}$ is linear and quadratic functions of u respectively.

In order to use an incremental solution procedure, the relation between du and $d\Psi$ must be found. Thus, taking appropriate variation of Equation (54) with respect to du :

$$d\Psi = \int_V dB^T \hat{\sigma} dV + \int_V B^T d\hat{\sigma} dV \quad (55)$$

where the variation of the external load with respect to displacements is equal to zero, and thus Equation (55) can be written at another form:

$$d\Psi = \int_V dB_L^T \hat{\sigma} dV + [\bar{K}] \quad (56)$$

where

$$[\bar{K}] = \int_A B^T D B dA = [K_o] + [K_L] \tag{57}$$

The first term of Equation (56) can be written as:

$$\int_V dB_L^T \bar{\sigma} dV = [K_\sigma] \tag{58}$$

where $[K_\sigma]$ is a symmetric matrix dependent on the stress level. This matrix is known as initial stress matrix or geometric matrix, thus,

$$d\Psi = ([K_o] + [K_L] + [K_\sigma]) du = [K_T] du \tag{59}$$

with $[K_T]$ being the total, or tangent stiffness matrix and $[K_o]$ is the constant linear elastic stiffness matrix and can be written as:

$$[K_o] = \int_A B_o^T D B_o dA \tag{60}$$

$[K_L]$ is the initial or large displacement matrix which is quadratically dependent upon displacement u , and can be written as [Pica and Wood, 1980]:

$$[K_L] = \int_A B_o^T D B_L dA + \int_A B_L^T D B_L dA + \int_A B_L^T D B_o dA \tag{61}$$

Finally $[K_\sigma]$ is the initial stress stiffness matrix which has to be found by using the definition of Equation (58). By taking the variation of Equation (51) then:

$$dB_L^T = \begin{bmatrix} \mathbf{0} & \mathbf{0} \\ dB_L^{bT} & \mathbf{0} \end{bmatrix} \tag{62}$$

This on substitution into Equations (58) and (37) gives:

$$[K_\sigma] = \int_A \begin{bmatrix} 0 & 0 \\ [G]^T d[A]^T & 0 \end{bmatrix} \begin{Bmatrix} N_x \\ N_y \\ N_{xy} \\ M_x \\ M_y \\ M_{xy} \end{Bmatrix} \tag{63}$$

However, using the mathematical properties of the matrix $[A]$, this matrix can be written as:

$$d[A]^T \begin{Bmatrix} N_x \\ N_y \\ N_{xy} \end{Bmatrix} = \begin{bmatrix} N_x & N_{xy} \\ N_{xy} & N_y \end{bmatrix} [G] da \tag{64}$$

and finally one can obtain

$$[K_{\sigma}] = \begin{bmatrix} 0 & 0 \\ 0 & [K_{\sigma}^b] \end{bmatrix} \quad (65)$$

Thus,

$$[K_{\sigma}] = \int_A [G]^T \begin{bmatrix} N_x & N_{xy} \\ N_{xy} & N_y \end{bmatrix} [G] da \quad (66)$$

It is recalled that the stresses resultants. In the present study, the imperfection is assumed to be of sinusoidal function over the plate as:

$$w_o(x, y) = w_o \sin\left(\frac{n\pi x}{a}\right) \sin\left(\frac{n\pi y}{b}\right) \quad (67)$$

The selective integration rule has been adopted to compute the integration of the matrices where (3×3) is used for bending and membrane energies and (2×2) for transverse shear energies.

The algorithm of the solution takes into account the nonlinearity in geometry of the element. The external load is applied incrementally and at every load increment the stiffness matrix of the plate is updated. The solution has been achieved by using the modified Newton-Raphson iterations technique. In the present study was used eight-node Serendipity element shown in **Figure 4**. This element contains four nodes at the corners, four nodes at the mid-sides of the element boundaries. The topology order is counter-clockwise in the sequence from 1 to 8 [Ammash, 2008].

NUMERICAL RESULTS AND DISCUSSION

A computer program has been developed, based on the foregoing finite element model to solve a number of numerical examples on the large displacement analysis of composite plate with variable spacing fiber under in-plane axial loading. Serendipity eight node element and five degree of freedom per node are used in the computations. Various boundary conditions, different aspect ratios, different slenderness ratios, different equations of distribution fibers were studied.

The material was used in the investigation consist from boron fibers with an epoxy matrix. Material properties are ($E_f=413.68\text{GPa}$, $E_m=3.44\text{GPa}$, $G_f=172.36\text{GPa}$, $G_m=1.277\text{GPa}$, $\nu_f=0.2$, and $\nu_m=0.35$) and the geometrical properties of the plate depends on the type of examples.

Seven different distributions of fibers were considered, each characterized by variations of the fiber volume fraction (V_f), as given in **Table 1**. These fiber distributions fall into two groups, having maximum values of V_f of 100% and 75%. **Table 1** also gives (V_{fav}), which is the average value of V_f for each distribution. That is,

$$V_{fav} = \int_0^a V_f(x) dx \quad (68)$$

Figure 5 shows the load-deflection curve of the simply supported laminated composite plate with variable fiber spacing under in-plane loading at x -direction obtained by using (2×2) mesh for the quarter plate. Seven equation of fiber distribution were used. This figure reveals the finite element results obtained by the eight-node isoparametric serendipity elements. In this example, the geometric properties of the analyzed plate are ($a=b=1.0$ m, $h=0.01$ m, $w_o/h=0.0$, $\theta = 0$). From this figure can be noticed that the post buckling behavior of composite plate very sensitive for type of distribution fiber and the seventh distribution equation in **Table 1** gives maximum buckling load and smallest deformation.

Figure 6 shows the load-deflection curve of the simply supported laminated composite plate with variable fiber spacing under in-plane loading at y -direction obtained by using (2×2) mesh for the quarter plate. Seven equation of fiber distribution were used. In this example, the geometric properties of the analyzed plate are ($a=b=1.0$ m, $h=0.01$ m, $w_o/h=0.0$, $\theta = 0$). From this figure can be noticed that the post buckling behavior of composite plate very sensitive for type of distribution fiber and the direction of uniaxial load. So the buckling load of the composite plate under in-plane loading at y -direction less than the buckling load of the composite plate under in-plane loading at x -direction about 14% for the seventh distribution equation. The seventh distribution equation gives maximum buckling load and smallest deformation.

Figure 7 shows the load-deflection curve of the simply supported laminated composite plate with variable fiber spacing under in-plane loading at x -direction. Seven equation of fiber distribution were used. The plate has initial imperfection (w_0/t) of (0.1) of which shape is considered to be sinusoidal curve where w_0 is the amplitude of the initial imperfection at center of plate. In this example, the geometric properties of the analyzed plate are ($a=b=1.0$ m, $h=0.01$ m, $w_0/h=0.1$, $\theta = 0$). From this figure can be noticed that the post buckling behavior of composite plate very sensitive for type of distribution fiber and to the initial imperfection.

Figure 8 shows the effect of fiber's orientation on the post buckling analysis of composite laminated plate with variable spacing fiber under in-plane compressive load. The seventh distribution fiber equation was used in this example. From this figure, it could be noticed that the post buckling of the plate with ($\theta=0^\circ$ and $\theta=90^\circ$) gives minimum deformation. This orientation's fiber means that it is the optimum for a plate under in-plane compressive load.

Figure 9 shows the effect of fiber's orientation on the post buckling analysis of composite laminated plate with variable spacing fiber under in-plane compressive load at x -direction. In this example, the geometric properties of the analyzed plate are ($a=b=1.0$ m, $h=0.01$ m, $w_0/h=0.1$). The all distribution fiber equations were used in this example. From this figure, it could be noticed that the post buckling of the plate with ($\theta=0^\circ$ and $\theta=90^\circ$) gives minimum deformation.

This orientation's fiber means that it is the optimum for a plate under in-plane compressive load. The proposed distribution equation represents optimum equation for the composite plate under in-plane loading.

CONCLUSIONS

It has been demonstrated that, for single layer plates having parallel fibers that are not densely packed, significant improvement in structural efficiency is obtainable by redistribution of the fibers so that they are concentrated more in the plate center where the fiber distribution may change the stiffness of the plate. The behavior of a laminated plate is very sensitive to the type of distribution fiber and it is found that the central deflection of a plate with ($\theta = 0^\circ$ and $\theta = 90^\circ$) gives response less than others; this orientation of fibers is optimum for plates under in-plane compression load.

REFERENCES

- Ammash, H. K., "Nonlinear Static and Dynamic Analysis of Laminated Plates Under In-lane Forces", Ph.D. Thesis, Engineering College, University of Babylon, Iraq, 2008.
- Leissa AW, and Martin AF., "Vibration and buckling of rectangular composite plates with variable fiber spacing", Compos. Struct., Vol.14, No.4, pp339–57, 1990.
- Leissa AW, Martin AF. "Some exact plane elasticity solutions for nonhomogeneous, orthotropic sheets", J Elastic , Vol.23, No.1, pp97–112, 1990.
- Martin AF, and Leissa AW., "Application of the Ritz method to plane elasticity problems for composite sheets with variable fiber spacing", Int. J. Numer. Methods Eng., Vol.28, No.(8), pp1813–1825,1989.
- Phan, N.D., and Reddy, J.N. "Analysis of Laminated Composite Plates Using a Higher Shear Deformation Theory" , Int. J. Num. Meth. Eng., Vol.21, pp. 2201-2219, 1985.
- Pica, A., Wood, R.D., and Hinton, E. "Finite Element Analysis of Geometrically Nonlinear Plate Behavior Using a Mindlin Formulation" , Comp. & Struct., Vol.11, pp.203-215, 1979.
- Pica, A., and Wood, R.D., "Post-Buckling Behavior of Plates and Shells Using a Mindlin Shallow Shell Formulation", Comp. & Struct., Vol.12, pp.759-768, 1980.
- Sheh-Yao Kuo, and Le-Chung Shiau, "Buckling and vibration of composite laminated plates with variable fiber spacing", Composite Structures, Vol.90, No.3, pp.196–200, 2009.

Shiau LC, and Chue Y.H.,“Free-edge stress reduction through fiber volume fraction variation”, Compos. Struct., Vol.19, No.2, pp.107–205, 1991.

Shiau LC, and Lee GC, “Stress concentration around holes in composite laminates with variable fiber spacing”,Compos Struct., Vol.24, No.2, pp.107-115,1993.

Table 1 Equations of fiber Distribution.

No.	$V_f(x)$	Volume fraction of fiber (%)	
		V_{fmax}	V_{fav}
1	$\left(\frac{4}{L}x - \frac{4}{L^2}x^2\right)$	100	66.67
2	$\left(\frac{4}{L}x - \frac{4}{L^2}x^2\right)^2$	100	53.34
3	$\left(\frac{4}{L}x - \frac{4}{L^2}x^2\right)^3$	100	45.70
4	$\frac{1}{2} + \left(\frac{1}{L}x - \frac{1}{L^2}x^2\right)$	75	66.67
5	$\frac{1}{2} + \left(\frac{1}{L}x - \frac{1}{L^2}x^2\right)^2$	75	63.34
6	$\frac{1}{2} + \left(\frac{1}{L}x - \frac{1}{L^2}x^2\right)^3$	75	61.42
7	$\left \sin\left(\frac{4\pi x}{L}\right)\right $	100	63.67

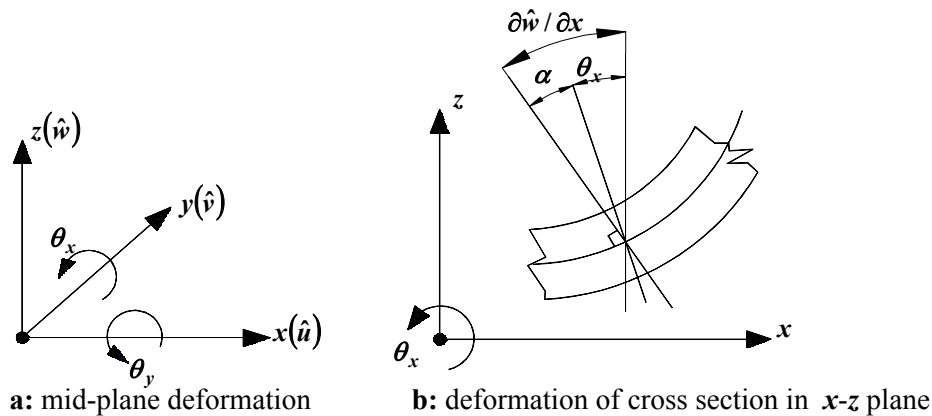


Figure 1 Deformations of moderately thick plate

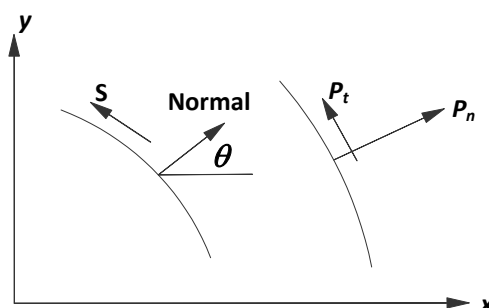


Figure 2 Edge tractions

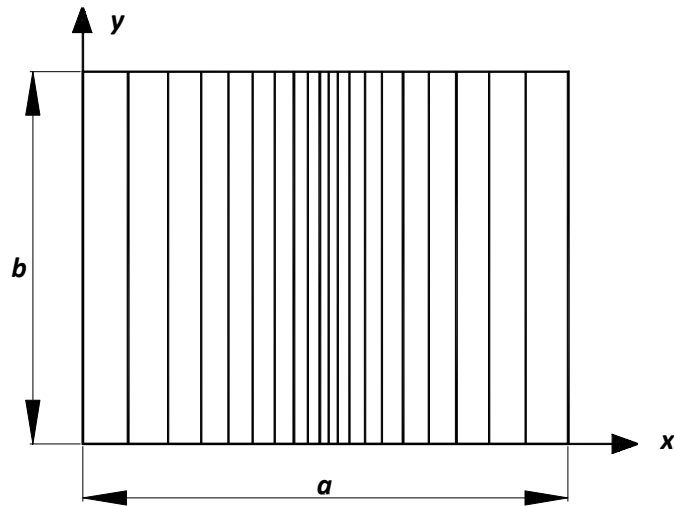


Figure 3 rectangular composite plates with variable fiber spacing.

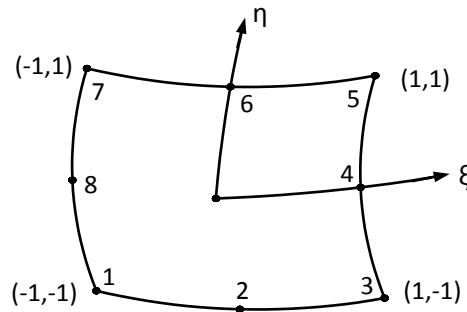


Figure 4 Eight-node quadrilateral isoparametric element.

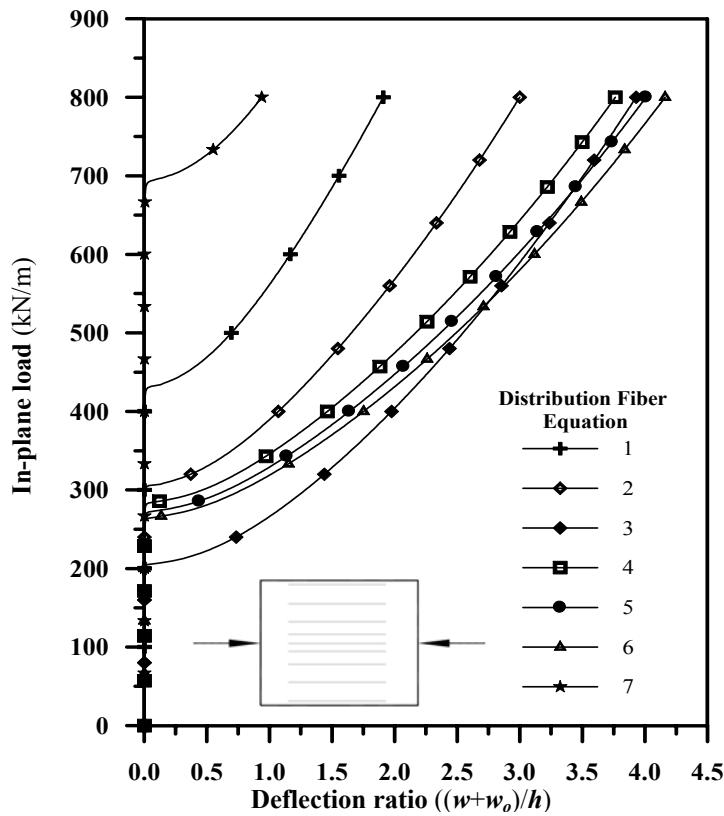


Figure 5 Post-buckling behavior of a square simply supported laminated composite plate with variable fiber spacing under uniaxial compression load x -direction.

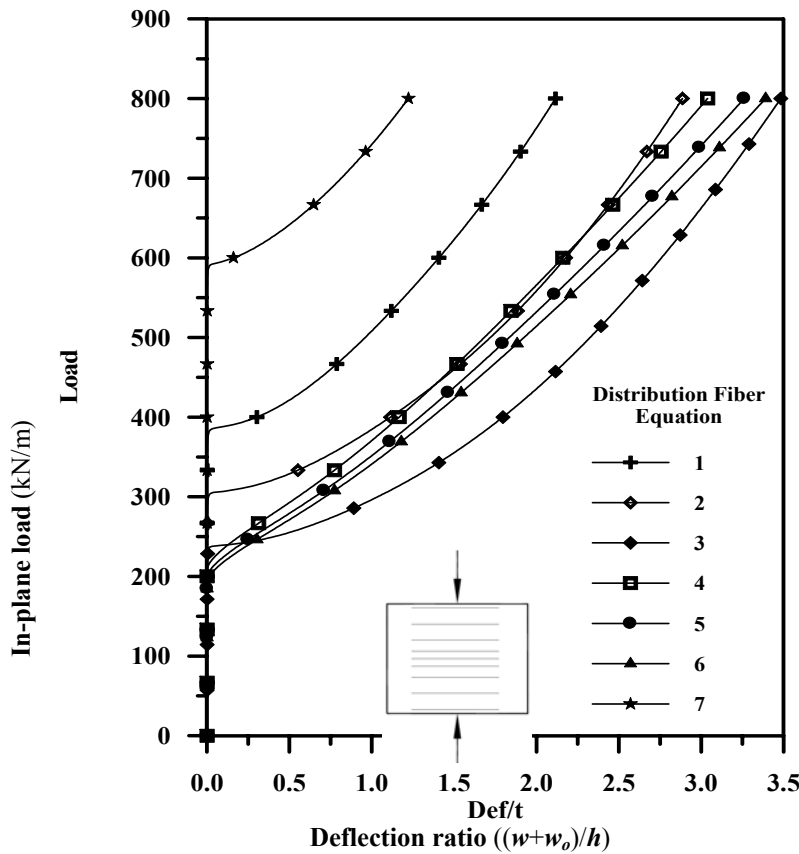


Figure 6 Post-buckling behavior of a square simply supported laminated composite plate with variable fiber spacing under uniaxial compression load *y*-direction.

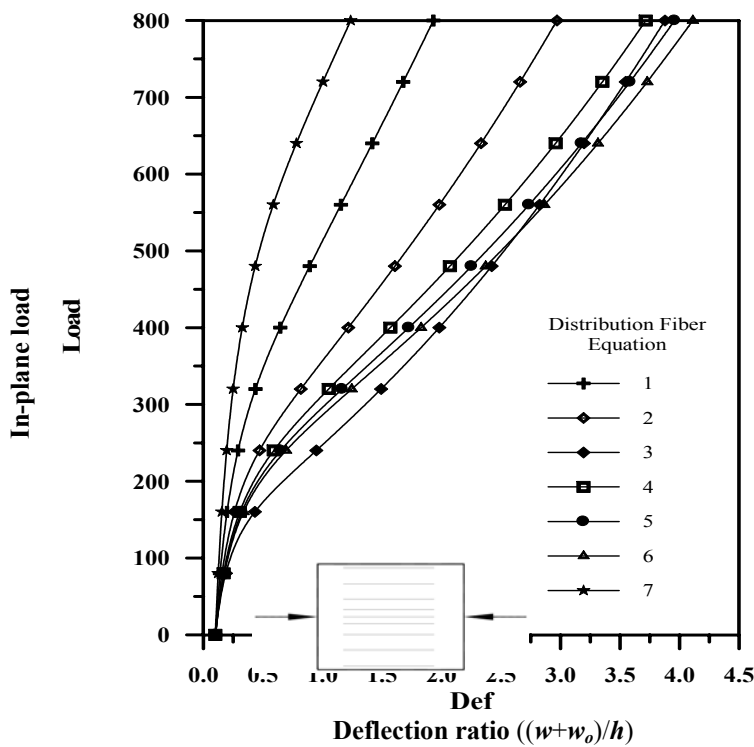


Figure 7 Post-buckling behavior of a square simply supported laminated composite plate with variable fiber spacing under in-plane loading at *x*-direction

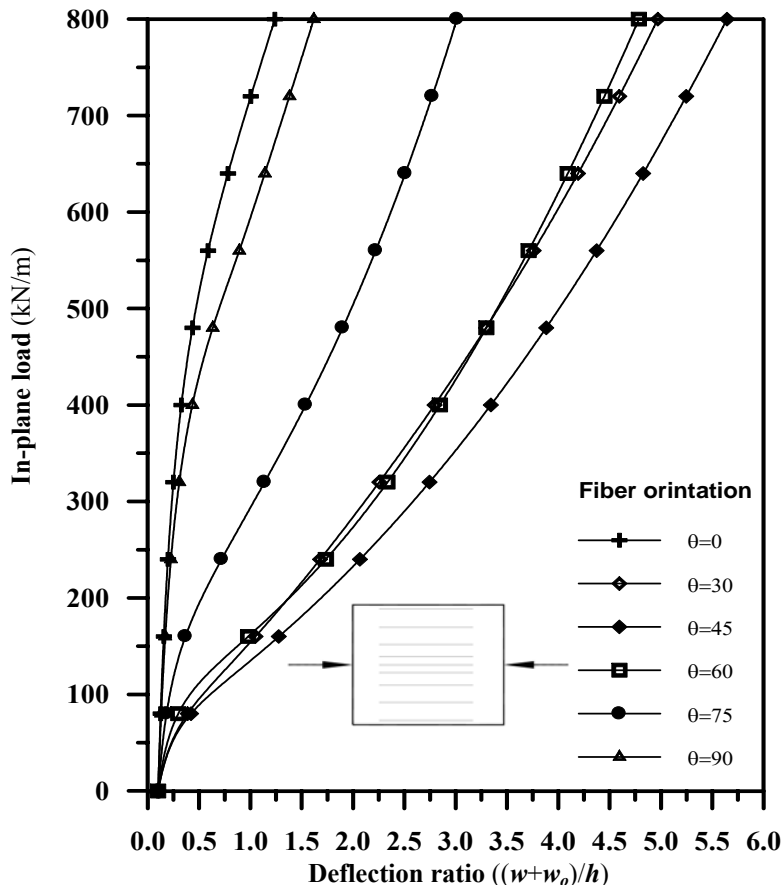


Figure 8 Post-buckling behavior of a square simply supported laminated composite plate with variable fiber spacing with various fiber orientations

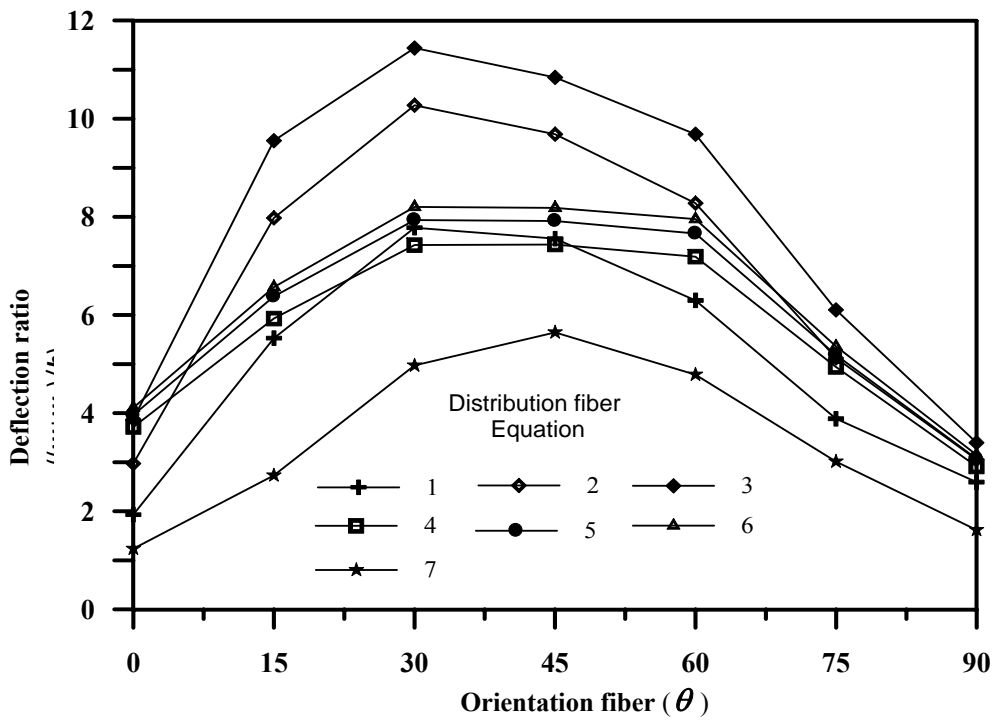


Figure 9 Deflection-orientation fiber curve of composite laminated plate under in-plane compression load at x-direction